J Eng Math (2006) 56:445–460
DOI 10.1007/s10665-006-9093-7

ORIGINAL PAPER

Lighthill and the triple-deck, separation and transition

Robert Bowles

Received: 21 July 2006 / Accepted: 31 August 2006 /
Published online: 13 October 2006

Abstract In 1953 James Lighthill, conducting an investigation into the potential mechanisms for upstream influence within boundary layers in supersonic flow, published a theoretical approach which explicitly took into account the influence of viscosity on a disturbance to an incident boundary-layer profile. In doing so he was able to predict a length-scale for upstream influence which scales with the global Reynolds number R, assumed large, as $R^{-3/8}$. The physical process he identified is now referred to as a pressure–displacement (or viscous–inviscid) interaction. This article discusses Lighthill's original paper and then proceeds to show how an appreciation of this interaction mechanism can help in the solution of many other problems in fluid mechanics and especially those of flow separation and late-stage laminar–turbulent transition. Finally, the article gives a brief description of the similarities between these two processes as seen from the unifying viewpoint of Lighthill's pressure–displacement interaction.

Keywords Lighthill · Pressure–displacement interaction · Separation · Transition · Triple-deck

1 Introduction

At the start of the 20th century Prandtl (1) introduced the concept of the boundary layer into fluid mechanics. The boundary-layer phenomenon is now central to many aspects of fluid mechanics, applied mathematics, engineering and much more and, of course, is a prime example of the method of matched asymptotic expansions as taught to undergraduate mathematicians. While successful in offering a possible resolution of d'Alembert's paradox—that the flow of a body through an unbounded inviscid fluid is drag-free—the adoption and increasing power of numerical methods to solve the boundary-layer equations showed by the middle of the century that boundary-layer theory itself had its own paradoxes.

Specifically use of the boundary-layer equations to study the initial development of the flow just downstream of an aligned flat plate led to the realisation of new issues within boundary-layer theory as it predicts an infinite wall-normal velocity at the trailing edge itself as shown by Goldstein in 1930 (2). The theory does a very good job in predicting the flow on the plate itself however. Goldstein also showed in 1948 (3) that for typical adverse pressure gradients, driving the boundary-layer equations towards flow separation,

R. Bowles (✉)
University College, Gower Street, London, SG99EQ, UK
e-mail: rob@math.ucl.ac.uk

the equations were subject to a singularity at the point of separation as had indeed been indicated by then-recent computations.

The explanation of the first of these paradoxes was clarified at the end of the 1960s in independent work by Stewartson (4), Messiter (5) and Neiland (6). The work of these authors led to the asymptotic structure known as the triple-deck. The second paradox was addressed by Stewartson (7) (see also his review paper (8)) and relates to the problem of large-scale separation from bluff bodies. Its resolution also requires the triple-deck structure which has found remarkable use since then, allowing significant progress to be made in the understanding of boundary-layer stability, both in a linearised study and in the fully nonlinear approaches required for a study of the transition to turbulence in such flows.

As the Reynolds number, $R \to \infty$, the length-scale of the triple-deck structure is $O(R^{-3/8})$ where $R = U_\infty l/\nu_\infty$ with U_∞ the free-stream velocity, used to nondimensionalise velocity, l the distance from the boundary-layer leading edge, used to nondimensionalise length and ν_∞ the kinematic viscosity in the free-stream. This special scale and its associated physical balances had been identified 15 years before the above formal presentations of the triple-deck, by James Lighthill in his 1953 paper "On boundary layers and upstream influence, II, Supersonic flows without separation." (9).

The current article is a review of recent developments in the application of high-Reynolds-number theory to problems in transition and unsteady separation, relating the work to Lighthill's paper. It starts with a commentary on the paper, and moves on to a brief description of the place of the triple-deck in the analysis of steady aerodynamic flows. It then turns to a more extended discussion of its application in the study of late-stage transition and unsteady separation. In particular, it discusses the similarities between the structures seen in computations of nonlinear planar Tollmien–Schlichting waves and of unsteady separation, as seen from a common theoretical viewpoint.

2 Lighthill's paper of 1953

2.1 The original paper

In 1953 James Lighthill examined the problem of predicting a boundary layer's response to a small disturbance, such as that caused by a weak shock in steady flow (9). Experiments had shown that the upstream extent of the response was typically of the order of tens of boundary-layer thicknesses and the paper was one of a series which tried to predict this length-scale theoretically. It was certainly an important technological problem at the time with the recent development of jet-powered and supersonic flight. The analysis he presented is for a compressible boundary layer, as necessitated by the particular motivating problem in the paper, but the mechanics he clarified can be active in incompressible flow also and the present discussion moves on to incompressible flow in due course.

The prime assumption of Prandtl's theory is that the boundary layer is thin relative to its streamwise length-scale so that cross-stream derivatives dominate over streamwise derivatives. The increased cross-stream velocity gradients are thus able to generate shear forces that balance the oncoming streamwise inertial forces, even at high Reynolds number. The thin layer is, however, unable to support cross-stream pressure gradients such as might be generated by significant streamline curvature. In addition, the streamwise pressure gradient driving the flow forward is prescribed by the solution to the inviscid equations governing the flow outside the boundary layer. This has the effect of rendering the boundary-layer equations parabolic.

The apparent adjustment seen upstream of the shock cannot therefore be calculated within Prandtl's boundary-layer theory. The problem of whether upstream influence is at all possible in supersonic flow vanishes when one realises that at the wall the fluid velocity is zero due to the no-slip boundary condition, so leading to a region of sub-sonic flow. Naturally therefore, investigators had concentrated on calculating the extent of the upstream influence over a streamwise length-scale comparable with the

boundary-layer thickness, thus allowing for cross-stream pressure gradients and perturbation vertical velocities commensurate with the streamwise perturbation velocities. So, although the problem involves the flow in a boundary layer, Prandtl's boundary-layer theory is not used, other than to determine the oncoming basic velocity profile close to the wall where the weak shock impinges. Over these shortened scales the weak influence of viscosity does not contribute to the dynamics of the flow, except in a thin wall layer which had hitherto been neglected. This was the approach taken by Lighthill in his prior consideration of the problem, published in 1950 (10). See also (11). The innovation in 1953 was to include the effects of this thin layer which, it turns out, has a crucial controlling influence on the upstream signature of the disturbance.

Lighthill solves the following inviscid equations for the pressure perturbation p and the ratio $\eta = v/\bar{U}$, where $\bar{U}$ is the base oncoming velocity profile, as determined by Prandtl's theory, and u and v the streamwise and cross-stream perturbation velocities, respectively:

$$p_x = \frac{\bar{M}^2}{1-\bar{M}^2}\eta_y, \quad p_y = -\bar{M}^2\eta_x, \tag{1}$$

$$u_x + v_y = 0, \tag{2}$$

where x and y are streamwise and wall-normal coordinates, respectively, and $\bar{M} = \bar{M}(y)$ is the Mach number profile. These imply that the pressure satisfies

$$\bar{M}^2\left(\bar{M}^{-2}p_y\right)_y + (1-\bar{M}^2)p_{xx} = 0. \tag{3}$$

These equations are not nondimensionalised or scaled in any way and arise from linearising the Navier–Stokes equations for a small perturbation about the oncoming boundary-layer profiles and neglecting the influence of viscosity.

The edge of the boundary layer is taken to be at the line $y = \delta$ where, in Lighthill's problem, the pressure distribution is given by the incoming and reflected shock and the reflected part is to be calculated. The boundary condition which is taken at the wall is the inviscid one $v = 0$, which leads directly to $p = 0$ when one also uses the fact that $\bar{M}(0) = 0$, as required by the no-slip condition. However, this predicts scales of upstream influence far less than those seen experimentally.

Lighthill uses Fourier transforms to represent the spatial variation of the solution and one can easily see in the presentation many of the ideas that he was later to promote in his monograph on Fourier Analysis (12). This enables him to make calculations of the details of the flow field generated by the incident shock and the reflection, the particular forcing of the boundary layer that he considers. However, the vital result from the paper with which we are concerned here is an expression for the logarithmic decrement of the decay of the upstream influence, which he refers to as κ_1. This is, of course, the least positive number such that $-\mathrm{i}\kappa_1$ is an eigenvalue for the unforced problem, in Fourier space, a point to which we return later.

The first step in extending earlier work is to assume an effective $\bar{M}(0) = \bar{M}_w$, other than zero, but otherwise small. The actual value of $\bar{M}_w$ emerges from subsequent calculations. Since close to the wall $\bar{M}$ increases linearly from zero, this is equivalent to applying the boundary condition not at the wall itself but close to it. This, in turn, can be identified as representing a vertical displacement of the oncoming Mach-number profile. It turns out that the effective displacement is not constant but depends on Fourier component and so on position. He then proceeds to show how the appropriate value of $\bar{M}_w$ can be calculated by considering the effect of viscous action on the perturbation velocities in an inner, viscous sub-layer where he insists that inertial effects are balanced by viscous effects. Due to the fact that this layer is thin and that the basic velocity profile there can be characterised by a constant shear, the calculation of the flow within this sub-layer is relatively straightforward, at least for a linearised disturbance. The Fourier transform $\hat{v}$ of the vertical velocity v in this viscous region satisfies

$$y\hat{v}'' = L^3\hat{v}'''', \quad L^3 = \frac{\nu_w}{\mathrm{i}k\lambda}, \tag{4}$$

i.e. Airy's equation for $\hat{v}'' = -ik\hat{u}'$, from the continuity equation. Again this is obtained from linearisation about the basic profile $\bar{U} = \lambda y$, $\bar{M} = \lambda y/a_w$ with λ the velocity gradient at the wall, a_w and ν_w the wall values of the sound speed and kinematic viscosity. Here k represents the Fourier component. The solution to (4) satisfying the appropriate boundary conditions is

$$\hat{v} = \int_0^y (y-q)\mathrm{Ai}(q/L)\,\mathrm{d}q, \tag{5}$$

with $\mathrm{Ai}(s)$ the Airy function satisfying $s\mathrm{Ai}(s) = \mathrm{Ai}''(s)$. Examining this solution for large y shows that its asymptote has a zero at $y = \Gamma L$ where

$$\Gamma = \frac{\int_0^\infty s\mathrm{Ai}(s)\,\mathrm{d}s}{\int_0^\infty \mathrm{Ai}(s)\,\mathrm{d}s} = \frac{-\mathrm{Ai}'(0)}{\int_0^\infty \mathrm{Ai}(s)\,\mathrm{d}s} = 0.78. \tag{6}$$

Looking at this solution from the perspective of the outer flow, Lighthill infers that the correct position to apply the boundary condition is at $y = \Gamma L$ so that $\bar{M}_w = \lambda\Gamma L/a_w$.

Solution of the Fourier transform of Eq. 3 with the free-stream boundary conditions applied at the boundary-layer edge and the wall conditions at $y = \Gamma L$ allows the transform of the solution to be found and hence the characteristics of the flow and the reflected shock to be made clear. Specifically it allows the length-scale of the upstream influence to be calculated as

$$\kappa_1^{-1} = \left(\frac{a_w}{a_\infty}\right)^{3/2}\left(\frac{\nu_\infty}{\nu_w}\right)^{1/4}\frac{l}{\Gamma^{3/4}(M_\infty^2-1)^{3/8}\tilde{\lambda}^{5/4}}R^{-3/8} \tag{7}$$

where we have introduced $\tilde{\lambda}$ (the velocity gradient at the wall, normalised with respect to $U_\infty/(lR^{-1/2})$, using $lR^{-1/2}$ an indication of the local boundary-layer thickness) so as to rewrite Lighthill's result slightly for the comparison which follows below.

The presentation of his analysis is perhaps not straightforward to follow for a modern reader who, maybe, has seen modern succinct presentations of the triple-deck structure beforehand but a "translation" is very easy to identify. So-called rational asymptotic methods and their application to fluid mechanics at high Reynolds numbers were developed in the late 1950s and 1960s, after Lighthill's paper; see work by Van Dyke (13), Kaplun (14), Lagerstrom and Cole (15), although Lighthill himself had contributed the method of strained coordinates in 1949 (16). Although every approximation Lighthill makes in his analysis is carefully justified, as well as being driven by exceptionally clear physical justification, they are not presented in the form of a rational asymptotic argument as might be expected now. For example he identifies a distinct boundary-layer edge at $y = \delta$ and applies boundary conditions for the equation for the perturbation pressure at this edge, rather than considering the free-stream and boundary layer as distinct outer and inner regions in a high-Reynolds-number expansion of the flow field between which solutions require matching. The boundary condition at the wall is not applied at the wall but at a small displacement from it whose value is calculated by including viscous terms close to the wall: this is an example of an approximation taken to be valid in one region of the flow field but actually corrected in another region, here a viscous wall layer. Such approximations would now be formalised in terms of matched asymptotic expansions.

The essential physical mechanism identified by Lighthill is easy to describe and it is important to realise that it exists regardless of the forcing of the boundary layer and independent of the Mach number. Close to the wall the flow is thickened (or indeed thinned) by some disturbance to the pressure distribution over a length-scale intermediate between the body-scale and the boundary-layer thickness. This thickening is controlled by viscous effects in the fluid and the no-slip condition and causes the flow immediately away from the wall to be pushed outwards or displaced. The pressure field caused by this displacement acts to drive the original wall layer. The length-scale of this so-called pressure–displacement interaction is identified in Lighthill's result (7) to be $O(R^{-3/8})$. At supersonic Mach numbers the mechanism allows an eigenvalue which gives rise to the exponential growth of the disturbance upstream of the forcing.

It is also active in sub-sonic flows, even though there is no eigenvalue in steady flow, and Messiter (5) and Stewartson (4) showed that it was able to describe the adjustment at a flat plate's trailing edge, a problem which we have seen is beyond Prandtl's theory. Since then it has found application in many other areas of fluid mechanics, including for example internal channel flow [17, 18] and hydraulic jumps [19, 20].

As the amplitude of the pressure disturbance increases, Lighthill's discussion of the importance of nonlinearity in the flow predicts a nonlinear response first occurs in the wall-layer when pressure disturbances reach $O(R^{-1/4})$. This nonlinearity can take the form of flow separation in the wall-layer.

2.2 An alternative approach

The more modern presentation of the same argument proceeds as follows. The Navier–Stokes equations are nondimensionalised with respect to the free-stream velocity, U_∞, distance from the leading edge, l and pressure $\rho_\infty U_\infty^2$ with the density in the free-stream ρ_∞. A physical argument, based on an understanding of the physical mechanism identifies the crucial length-scale as $O(R^{-3/8})$ and x is scaled as $x = R^{-3/8}X$. Two asymptotic regions can then be seen to arise from Eq. 3, one which has $y = O(R^{-3/8})$ also and a second in which $y = O(R^{-1/2})$, the local boundary-layer thickness. We will presume the amplitude of the pressure disturbance in the free stream to be $O(R^{-1/4})$, sufficient as we have seen to possibly provoke separation and write it as $R^{-1/4}\bar{P}$. To examine the first of the asymptotic regions in (3), we write $y = O(R^{-3/8})\bar{y}$ and the Navier–Stokes equations then yield

$$\bar{P}_{\bar{y}\bar{y}} + (1 - M_\infty^2)\bar{P}_{XX} = 0. \tag{8}$$

This region lies outside the boundary layer and the Mach number is seen to take its free-stream value. It is referred to as the outer deck.

The solution to (8) for the pressure perturbation and for the associated vertical velocity, $R^{-1/4}v$, again in terms of Fourier components, is

$$\hat{\bar{P}} = \hat{P}\exp(-\mathrm{i}k\beta\bar{y}), \quad \hat{v} = \beta\hat{P}\exp(-\mathrm{i}k\beta\bar{y}), \tag{9}$$

for an unknown $\hat{P}(k)$. Here we have allowed outgoing disturbances only in the supersonic free-stream, in contrast to Lighthill who considers an incoming shock. The region with $y = O(R^{-1/2})$ in (3) covers the boundary-layer thickness and as a result cross-stream derivatives dominate over streamwise ones and (4) simplifies to

$$\bar{M}^2(\bar{M}^{-2}P_{\tilde{y}})_{\tilde{y}} = 0, \tag{10}$$

where $y = R^{-1/2}\tilde{y}$. The solution is,

$$P_{\tilde{y}} = R^{-1/8}A_{XX}\bar{M}^2, \quad v = -A_X\bar{U}, \tag{11}$$

where we have chosen the unknown function of X introduced on integration of (10) to be $R^{-1/8}A_{XX}$ to agree with the modern usage of $A(X)$ as the negative displacement function. The continuity equation gives the perturbation streamwise velocity to be $R^{-1/8}u$, with

$$u = A\bar{U}'. \tag{12}$$

The first two terms in the expansion for the streamwise velocity are therefore

$$U = \bar{U}(y) + R^{-1/8}A(X)\bar{U}'(y) + \cdots = \bar{U}(y + R^{-1/8}A) + \cdots, \tag{13}$$

so that $-R^{-1/8}A(X)$ corresponds to a vertical displacement of the oncoming velocity profile. This asymptotic region, known as the middle deck, is able to support a cross-stream variation in the normalised pressure, P, of order $R^{-1/8}$ only, so that the pressure throughout the region is $R^{-1/4}P(X)$, obtained by evaluating (9) at $\bar{y} = 0$. Matching the solutions for v in (9) and (10) yields the result

$$\beta P = -A_X, \tag{14}$$

which is now referred to as the pressure–displacement law for supersonic flow and is Ackeret's Law. It represents the inviscid response of the flow to the profile's displacement.

Lighthill considers the behaviour of v in the viscous wall layer, now referred to as the lower deck, but it is now more common to examine u. As $\tilde{y} \to 0$, approaching the viscous layer, $v \to 0$, but the displacement A causes a slip velocity $R^{-1/8}\tilde{\lambda}A$. The slip needs to be reduced to zero by the wall layer and this gives a second constraint between the pressure and the displacement. This region has $y = R^{-5/8}Y$, a thickness scaling that can also be found in Lighthill's paper, and the equations for the perturbation streamwise and wall-normal velocities $R^{-1/8}U$ and $R^{-5/8}V$ are

$$(UU_X + VU_Y) = -(\rho_w/\rho_\infty)P_X + (\nu_w/\nu_\infty)U_{YY}, \quad U_X + V_Y = 0,$$
$$\text{with} \quad U = V = 0, \text{ on } Y = 0, \quad U \to \tilde{\lambda}(Y + A) \text{ as } Y \to \infty, \tag{15}$$

to match with the middle deck. Here ρ_w is the fluid density at the wall. The nonlinear system (15), when taken with (14), relating the unknown pressure and displacement, is of the boundary-layer type, but the driving pressure is not prescribed as in Prandtl's theory. For relatively small disturbances (15) can be linearised about the basic flow $U = \tilde{\lambda}Y$ and, using Fourier transforms and differentiation in Y, gives Airy's equation for the perturbation $\hat{u}'$, with a prime denoting differentiation with respect to Y:

$$Y\hat{u}' = \tilde{L}^3 u''', \quad \tilde{L}^3 = \nu_w/\mathrm{i}k\tilde{\lambda}\nu_\infty. \tag{16}$$

So matching the solution for $\hat{u}$ with the middle deck's solution yields

$$\hat{u}(Y) = \tilde{\lambda}\hat{A}\int_0^Y \mathrm{Ai}(q/\tilde{L})\mathrm{d}q \Big/ \int_0^\infty \mathrm{Ai}(q/\tilde{L})\mathrm{d}q. \tag{17}$$

Finally, we obtain a second expression relating the pressure and displacement from the derivative of (17) at $Y = 0$, where from (15) $\rho_w \mathrm{i}k\hat{P}/\rho_\infty = \nu_w\hat{u}''/\nu_\infty$, to give

$$\rho_w \mathrm{i}k\hat{P}/\rho_\infty = \frac{\nu_w\lambda\mathrm{Ai}'(0)}{\nu_\infty\tilde{L}^2\int_0^\infty \mathrm{Ai}(q)\mathrm{d}q}\hat{A} = -\frac{\Gamma\nu_w\lambda}{\nu_\infty\tilde{L}^2}\hat{A}. \tag{18}$$

Alternatively, this result may be obtained by examining (15) as $Y \to \infty$ which is closer to Lighthill's approach. Combining (14) and (18) leads to the result for $k = -\mathrm{i}\tilde{\kappa}_1$ with

$$\tilde{\kappa}^{-1} = \left(\frac{\rho_\infty}{\rho_w}\right)^{3/4}\left(\frac{\nu_\infty}{\nu_w}\right)^{1/4}\frac{l}{\Gamma^{3/4}(M_\infty^2 - 1)^{3/8}\tilde{\lambda}^{5/4}}, \tag{19}$$

agreeing with Lighthill's (7), given that $(a_w/a_\infty)^2 = \rho_\infty/\rho_w$.

We may factor out the constants $\tilde{\lambda}$, β, ν_w/ν_∞, ρ_∞/ρ_w from the above presentation by redefining the flow variables and the relevant canonical triple-deck equations are then

$$UU_X + VU_Y = -P_X + U_{YY}, \tag{20}$$

$$U_X + V_Y = 0, \tag{21}$$

$$U = V = 0, \text{ on } Y = 0, \quad U \to Y + A, \text{ as } Y \to \infty, \tag{22}$$

$$P = -A_X \quad \text{or} \quad P = \frac{1}{\pi}\int_{-\infty}^{\infty}\frac{A_S}{X - S}\mathrm{d}S, \tag{23}$$

according to whether the flow is supersonic or subsonic. These flow problems are now unforced, so that one solution is simply $V = P = A = 0$, $U = Y$. However, we have seen that in the supersonic case an eigensolution is possible which grows as it develops downstream. As it reaches sufficient amplitude, separation occurs and the far-downstream solution has a separated shear layer with a slow returning flow beneath (21). An exactly analogous solution is possible in the subsonic case (22). Above all here, these equations capture the pressure–displacement interaction first identified by Lighthill.

3 Flow separation

3.1 Steady boundary layers in an adverse pressure gradient. Large-scale separation

As we have discussed in Sect. 1 above, the steady boundary-layer equations are subject to a singularity, the Goldstein singularity, when separation is approached in a region of adverse pressure gradient. Like the trailing-edge problem, which the interactive boundary-layer equations are able to resolve, the singularity has a signature of large vertical velocities. Goldstein (3) shows that the vertical velocity behaves like $(x_s - x)^{-1/2}$ as the position of the singularity, x_s, is approached. However, in contrast to the trailing-edge problem, and as shown by Stewartson (7), there appears to be in general no way that the solution can be continued through the singularity, at least by the introduction of an interactive boundary-layer system over a shortened length-scale. We are forced to conclude that the driving pressure gradient, fixed by the inviscid solution exterior to the boundary layer and calculated on the assumption that the boundary layer does not separate, is incorrect. Instead, the boundary layer does separate at some point on the surface and the problem of predicting that point requires a global consideration of the large-scale properties of the flow, the separated region and the pressure gradient driving the boundary layer upstream of separation, that Prandtl's theory predicts for this new effective body shape. The triple-deck structure and the $R^{-3/8}$ length-scale still have a vital role to play in this calculation as they are capable of describing the breakaway separation of the boundary layer, the separation process itself, although the position of separation must be found from properties of the global problem; see (8,23).

4 The addition of unsteadiness—Boundary-layer stability

4.1 Lower-branch stability and the $R^{-3/8}$ length-scale

The triple-deck structure has found great application in the study of steady flow. However, at high values of the Reynolds number flows are generally unsteady and turbulent and the study of the transition to turbulent flow is of technological importance. The pressure–displacement interaction has had application to this nonlinear stability problem also.

The study of the stability of a Blasius boundary-layer profile to linearised wave disturbances leads to the Orr–Sommerfeld equation which needs to be solved to give the dispersion relation. At high Reynolds numbers the flow is unstable to a range of frequencies marked at its lower and upper edges by the so called lower- and upper-branch neutral curves. The features of the disturbance at high Reynolds numbers were established by Tollmien (24) and Lin (25) and it was known at the time of Lighthill's paper that neutral disturbances on the lower-branch have a length-scale that scales with $R^{-3/8}$ as $R \to \infty$, precisely the upstream influence scale which he identified.

That the triple-deck structure could be used to study the stability of the boundary layer was first realised by Smith [26, 27], 25 years after Lighthill's work. One wonders why Lighthill did not explicitly make the connection himself. Although he did not publish widely in the field of flow stability, he does give a clear description of the mechanism of the Tollmien–Schlichting wave in the book edited by Rosenhead (28, Part II, Sect. 3.1). This describes the wave in terms of a vertical advection, or displacement, of the vorticity in the boundary layer allied with a destabilising influence of viscosity generated in a wall layer. Reading this description with his 1953 paper in mind makes it perhaps surprising that he did not explicitly make the connection himself.

4.2 Nonlinear disturbances, spiking and transition

The advantage that the triple-deck structure offers the investigator into boundary-layer stability, along with its "rational approach", is that it leads to a nonlinear description of the flow and full transition to

turbulence is a nonlinear mechanism. The time-scales of the lower-branch disturbances is such that their high-Reynolds-number structure are captured by simply replacing the left-hand side of (20) by

$$U_T + UU_X + VU_Y. \tag{24}$$

Transition is also a highly three-dimensional process in reality. Analysis of the three-dimensional analogue of this new unsteady system has revealed much about the nonlinear processes that can be present in transitional flows for lower-branch disturbances [29–32]. However, perhaps the most universal feature of transition to turbulent flow is the breakdown of the flow to smaller space- and time-scales and particularly the occurrence of "spikes", short-scaled and large-amplitude events in a measurement of the disturbance velocity against time. These indicate the start of late transition and have been seen in many experimental and computational studies and at the end of various routes through early transition [33–36]. A theoretical approach, starting with the two-dimensional unsteady interactive equations (20–24) has been developed in [37–42] and which has its origins in the wave-breaking singularity suggested by the form of the streamwise momentum terms (24). See (43, Chapter 2) and (44, Chapter 2). The shortening length-scales associated with such a singularity generate enlarged vertical velocities and so an increased displacement might be expected. However, Reference (37) shows that under certain conditions the vertical velocity does not grow as one moves out of the lower-deck and as a result the pressure that is generated by the displacement effect is not large enough to feed back onto the basic wave-breaking structure. This condition on the streamwise velocity profile is

$$\int_0^\infty \frac{\mathrm{d}Y}{(\bar{U}-c)^2} = 0, \tag{25}$$

where the integral is to be interpreted as a generalised principal value and the velocity profile $\bar{U}$ has an inflection point at $y = y_c$, so that $\bar{U}''(y_c) = 0$ and $c = \bar{U}(y_c)$. In (38) this condition is put forward as a criterion for the onset of late-stage transition, as it allows for shortened space- and time–scales to emerge naturally from the development of solutions to (20–24). Although the satisfaction of this condition effectively breaks the feedback allowed by the pressure–displacement interaction, the interaction is still vitally important in that the pressure driving the flow within the boundary layer is free to emerge from the dynamics at play there as opposed to being fixed by some external inviscid flow as in Prandtl's theory.

As length-scales shorten, the effects of the increased wall-normal velocities and the wall-normal pressure gradients they provoke do become physically significant. In (39) it is shown that the governing equation for the disturbance pressure, $\tilde{P}$, in a frame travelling downstream with speed c is, in normalised terms,

$$\tilde{P}_T + \tilde{P}\tilde{P}_X = \frac{1}{\pi}\int_{-\infty}^{\infty} \frac{\tilde{P}_{SS}\mathrm{d}S}{X-S} + \mu J_X. \tag{26}$$

The term J_X arises from the solution in the critical layer, centred on $y = y_c$. The length-scale over which the pressure disturbance is controlled by this equation is $O(R^{-9/16})$ which is shorter than the original interactive or Tollmien–Schlichting scale of $O(R^{-3/8})$.

A solution of (26) for $\mu = 0$ and with initial conditions corresponding to the wave-breaking process is presented in Fig. 1. It shows the generation of maxima and minima in the pressure trace as the dispersive integral term grows in importance. In fact, the critical-layer term J_X grows arbitrarily large locally as a pressure max/min pair is first generated. However, examination of the processes at work in the critical layer at this point in the flow's development in (41) indicates that this corresponds to the generation of a vortex, a region of trapped recirculating fluid, and in the limiting case of small values of μ the solution can be continued through this stage to yield a pressure distribution containing a string of max/min pairs and associated vortices (42).

The mechanisms at work above are essentially inviscid as the time- and space-scales are so short. Viscous influences are of course required to satisfy the no-slip condition in a thin wall layer but, as the frame in which (26) is valid passes downstream sufficiently rapidly, there is very little interaction between the flow

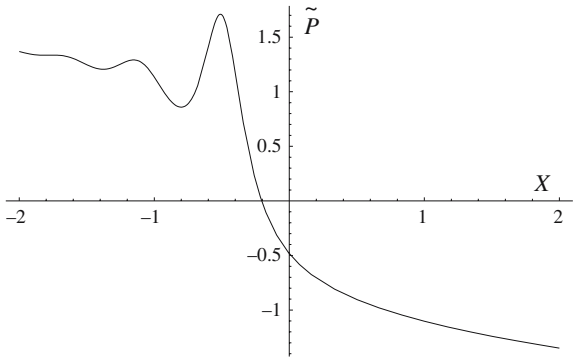

Fig. 1 The theoretical prediction for the streamwise pressure distribution obtained through a solution of (26) with $\mu = 0$ and suitable initial conditions; see (39). Compare with the distributions in the simulations in Fig. 4

in that thin wall layer and the wave-breaking processes. Nevertheless the large skin friction generated at the wall by the increasing streamwise pressure gradient is one of the first indicators of the wave-breaking process occurring.

The development of this theoretical approach is continuing with the study of three-dimensional effects within the critical layer (45) and alternative transition routes following the development of a profile satisfying (25) (46). This approach to the study of transition has been successful in terms of the theory's self-consistency and its provision of physical insight, through the prediction of active scales and physical mechanisms and its broad agreement with direct numerical simulations and three-dimensional experiments. Another area of continuing research concerns high disturbance environments and here Ryzhov's (47) prediction of the transition length-scale to be $O(R^{-3/8})$ is of particular interest.

4.3 Comparison with planar computations

Detailed qualitative comparisons of the preceding theoretical approach and careful numerical simulations of a large-amplitude two-dimensional train of Tollmien–Schlichting waves are made in (48) and we summarise the results of this comparison here in Figs. 2–5. The Reynolds number of these computations is Re = 2,500 based on boundary-layer thickness, so that $R = O(\mathrm{Re}^2)$, and the boundary layer is forced by a suction/blowing strip, turned on smoothly to start the calculation. A wave-train of Tollmien–Schlichting waves is seen to develop as shown in Fig. 2. The amplitude of the disturbance is sufficient to cause separation downstream from $x = 280$, as shown in Fig. 2b. We are also able to see short-scaled events just upstream of these separated flow regions and we identify these events as the predicted wave-breaking events. They develop finer structure further downstream and perhaps the most obvious feature is the large values of wall vorticity within the events, again as predicted. A closer view of the pressure profile in one of these events is given in Fig. 3 which also gives a line contour plot of the vorticity within the flow, Ω, and a shaded contour plot of the vertical velocity. We note that there is a region of positive vertical velocity at $x = 315$, $y = 0.5$ and that this acts to convect upwards the negative values of vorticity, emanating in the separated region and advected upstream in the frame of the wave as it passes downstream. This vertical velocity is caused by the local shortening of length-scale through the wave-breaking singularity. Subsequent development of the disturbance is illustrated in Fig. 4 in a similar fashion to that in Fig. 3. A localised pressure max/min pair has developed, causing the finer structure mentioned above, and the contours of vorticity clearly show the development of a vortex, at $x = 442$, $y = 0.8$. Associated with this vortex is a patch of downward wall-normal velocity. This is precisely as predicted by the theory and the computation shown in Fig. 1. Indeed computations

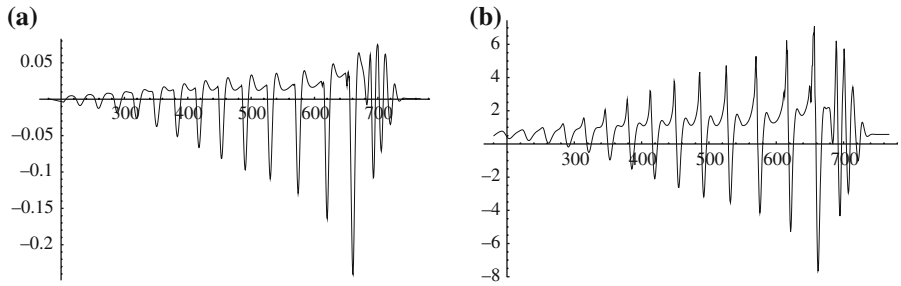

Fig. 2 The wave-train of Tollmien–Schlichting waves at Re = 2,500. The forcing is centred about $x = 160$. (**a**) Wall pressure $p(x, 0)$. (**b**) Wall vorticity $\Omega(x, 0)$

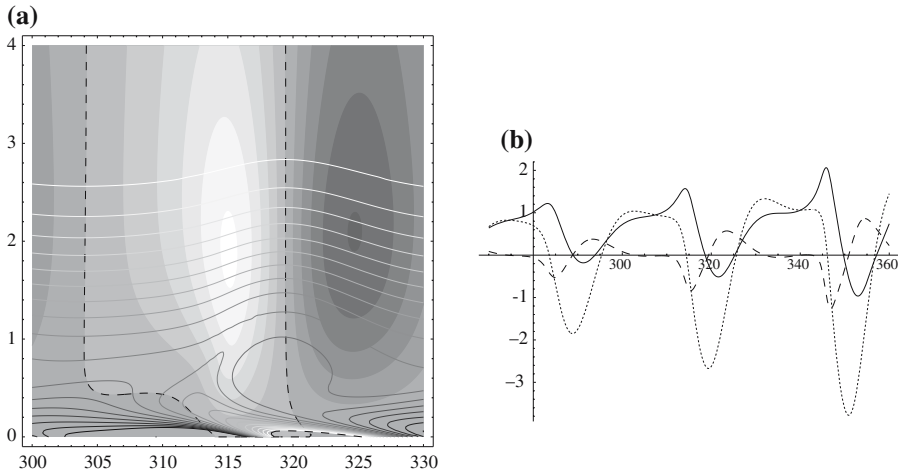

Fig. 3 The early development of the spike at $x = 315$, Re = 2,500. (**a**) Line contours of the vorticity Ω in the range 0.05 (white) to 0.8 (black) in steps of 0.05 with the additional zero contour dashed. The vertical velocity v is denoted by the shading with contour values −0.25 (darkest) to 0.25 (lightest) in steps of 0.05 with a dashed zero contour. (**b**) Wall vorticity (solid), wall pressure $500P(x, 0)$ (dotted) and pressure gradient $500P_x(x, 0)$ (dashed)

at higher Reynolds number presented in (48) show more vortices and more pressure maxima. At the lower Reynolds number of the current computations viscosity is able to arrest the development of further vortices. The continued development of the flow is presented in Fig. 5. The vortex has now grown significantly but the striking feature is evidence of a secondary eruption of vorticity from close to the wall at $x = 534 - 535$. This looks broadly similar to the original spike in vorticity seen in Fig. 3 but reversed in a streamwise sense and one is tempted to see this as the start of a cascade of wall-eruptions. However, there is a difference in that the eruption is of high values of vorticity, generated as the initial signal of the spike, being advected vertically through a region of reduced vorticity. The spike seen in Fig. 3 was of reduced vorticity passing through higher values. Theoretically this would be reflected by a change in the sign of μ in (26) and it is interesting to note that (39) finds, in that case, that (26) is ill-posed and unstable. This might explain the wave-packet-like signal in the wall pressure seen in Fig. 5b.

The capture of such secondary eruptions of vorticity from wall-layers is beyond the scope of the theory as presented in Sect. 4.2 which predicts linearised behaviour within the wall layer and hence no separation and allows for no interaction between the developing pressure profile and the flow at the wall. This is a point to which we return below in Sect. 5.3.

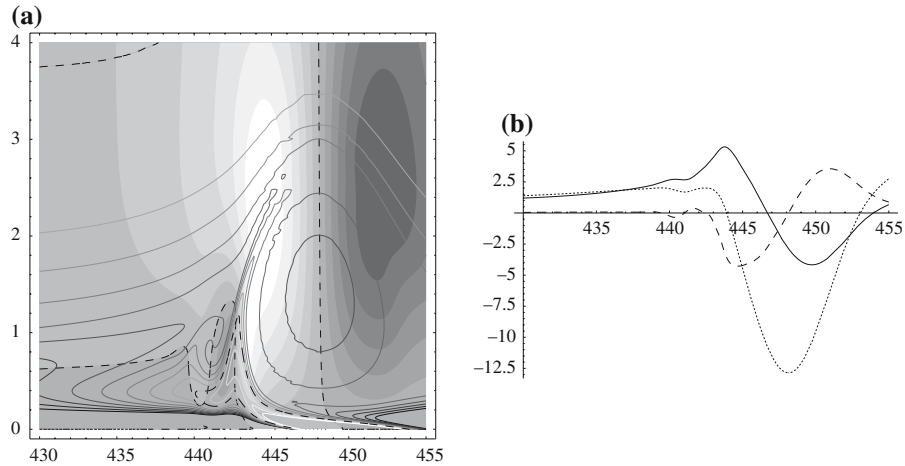

Fig. 4 The continued development of the spike at Re = 2,500 showing vortex generation and pressure max/min. (**a**) Line contours of the vorticity Ω in the range −0.4 (white) to 0.8 (black) in steps of 0.1 with the additional zero contour dashed. The vertical velocity v is denoted by the shading with contour values −0.1 (darkest) to 0.1 (lightest) in steps of 0.02 with a dashed zero contour. (**b**) Wall vorticity (solid), wall pressure $100P(x,0)$ (dotted) and pressure gradient $100P_x(x,0)$ (dashed)

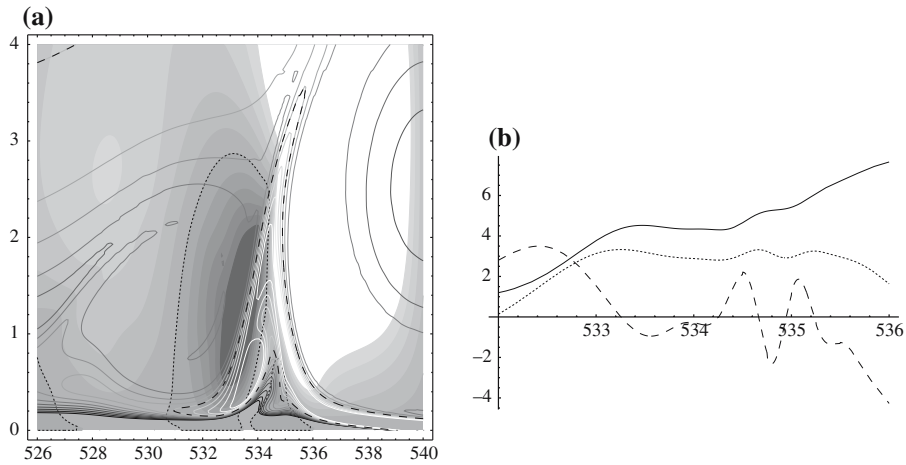

Fig. 5 Secondary eruptions from the wall layer. (**a**) Line contours of the vorticity Ω in the range −0.4 (white) to 0.6 (black) in steps of 0.05 with the additional zero contour dashed. The vertical velocity v is denoted by the shading with contour values −0.1 (darkest) to 0.1 (lightest) in steps of 0.01 with a dashed zero contour. (**b**) Wall vorticity (solid), wall pressure $100P(x,0)$ (dotted) and pressure gradient $100P_x(x,0)$ (dashed)

5 Unsteady separation

5.1 Aspects of the high-Reynolds-number theory of unsteady separation

Another area of fluid dynamics where the concept of a pressure–displacement interaction has a role to play is in the understanding of unsteady separation. We have seen that Prandtl's boundary-layer theory is not successful in predicting steady separation from bluff bodies and it is natural to investigate the unsteady boundary-layer equations to try to investigate how a steady separated flow might be set up. If a body is started impulsively, then the unsteady version of the boundary-layer equations actually has a steady prescribed pressure gradient, established over a time-scale shorter than the viscous time-scale over which the boundary layer can develop, and has inertial terms given by (24). Experimentally for a cylinder the

boundary layer is seen to separate from the body after a relatively short time at a point approximately three quarters of the way around from the leading stagnation point but, instead of describing this separation process, integration of the unsteady boundary-layer equations terminates in a finite-time singularity [49–51]. Physically the singularity arises as fluid particles bunch together in the streamwise direction as they decelerate typically on the rear portion of the bluff body. This in turn leads to a thickening of the boundary layer and large vertical velocities. Within the context of Prandtl's boundary-layer equations these velocities grow without limit as there is no acting cross-stream pressure gradient. By considering the possibility of a pressure–displacement interaction with a pressure gradient provoked by the increasing boundary-layer displacement (52) show that an interactive system is established as the singularity time is approached. The importance of this is that it is now susceptible to the same wave-breaking singularity and subsequent development as described in Sect. 4.2, although (53) demonstrate that the system is subject to a rapidly growing inviscid instability.

5.2 Finite-Reynolds-number computations of unsteady separation

However, at finite Reynolds number a development as clear as predicted above is not necessarily seen. The flow develops differently and indeed it seems that for finite but sufficiently large Reynolds number an entirely alternative development is possible, one with more pressure–displacement interaction in fact. Computations of the planar Navier–Stokes equations for the flow induced by a vortex moving in a mean flow close to a wall have been carried out in [54–58] and others. Such a problem is of inherent interest in the study of transitional and turbulent wall-bounded flow where such interactions are common and play an important role in maintaining the turbulence but the problem has shed much light on the study of unsteady separation. A clear discussion of the comparison between these computations and theory is given by Cassel (55) and the computations follow the complete flow field including the vortex and the thin viscous wall-layer that is generated as it passes and of course any subsequent interaction. For our purposes we are interested in the development of the wall layer. For early times the flow is as predicted by Prandtl's theory. However, a pressure–displacement interaction, referred to as a "large-scale interaction", is seen to develop *before* significant eruption of the wall-layer as predicted by van-Dommelen's singularity. This is detected as a departure of the wall-pressure from that which would be generated by the inviscid flow outside the wall-layer by the passing vortex. For a relatively low Reynolds number, Re, based on the advection velocity of the vortex and the distance of the vortex centre from the wall, of 10^3, the flow in the boundary layer does not develop further. For $\mathrm{Re} = 10^4$ or 10^5 a "short-scale interaction" is also subsequently seen to develop which has a signature of large pressure gradients and wall vorticity and Cassel identifies this with the wave-breaking singularity described in Sect. 4.2. A measurement of the maximum values of wall-normal pressure gradient shows that these grow significantly within this interaction at a time when localised pressure max/min pairs are generated. It is interesting to note that, at these finite Reynolds numbers, this complete process can be identified before the time at which Prandtl's theory would fail due to the van-Dommelen singularity. The interactive boundary-layer theory, which strictly is based on the assumption of infinite Reynolds number predicts physical balances and effects that are in fact active at lower Reynolds numbers and which may be seen before the breakdown inherent in the non-interactive theory.

More recent computations at higher Reynolds numbers still (56,58,59) suggest that instabilities can grow within these complicated flows. Instabilities that might be related to the one predicted in (53) are discussed in (56,58). Alternative Rayleigh instabilities in the flow, which arise as soon as an inflection point is generated in the velocity profiles close to the wall, are able to grow at still higher Reynolds numbers as discussed in (59) and for $R = 10^7$ they occur even before the large-scale interaction is established. See the theoretical work (60) in this respect and also (61).

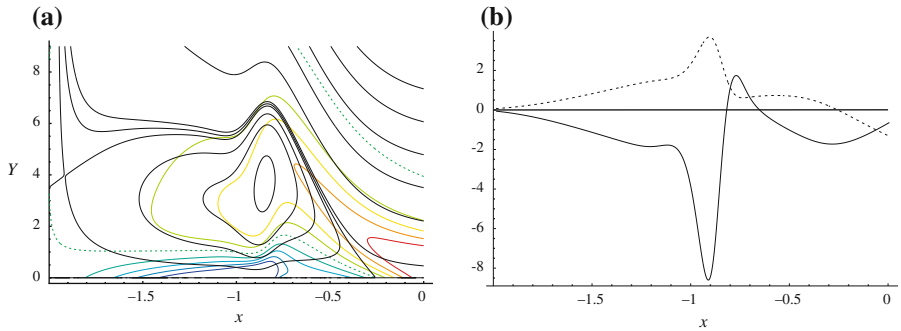

Fig. 6 The early development of the large-scale interaction (57). (**a**) Streamlines and contours of vorticity. (**b**) Wall shear stress (dashed) and pressure gradient (solid)

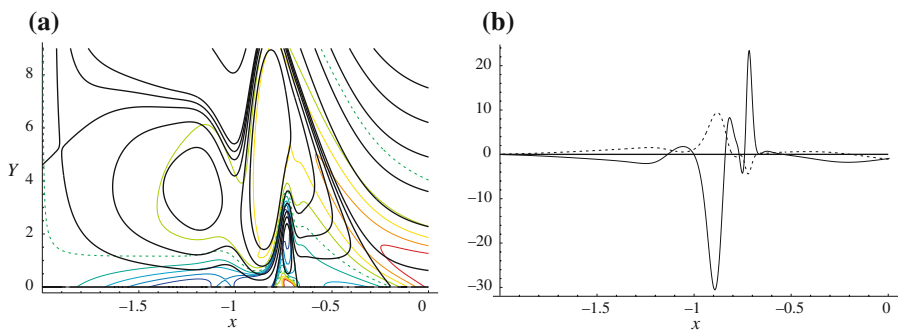

Fig. 7 The later development of the large-scale interaction (57). (**a**) Streamlines and contours of vorticity. (**b**) Wall shear stress (dashed) and pressure gradient (solid)

5.3 The similarities between separating and transitional flows

It is worth considering the similarities between these vortex-induced flows and the short-scaled events occurring in the large-amplitude Tollmien–Schlichting wave-train described in Sect. 4.3. Figures 6 and 7 are taken from (54) and show streamlines and vorticity contours close to the wall together with plots of wall vorticity and pressure gradient. The large-scale interaction is illustrated in Fig. 6 in which the flow away from the wall is from right to left, decelerating as it goes, and the flow closer to the wall is separated between $x = 0$ and $x = -0.2$ approximately. The interaction takes place around $x = -0.8$ and is marked by increasing values of wall vorticity. The subsequent development is shown in Fig. 7 and we can see two additional features. First, the recirculating separated region has been split at $x = -1$ and second there has been an eruption of the large values of wall vorticity into the near-wall flow.

The similarities with Figs. 3 to 5 are strong although the physical contexts differ. For example the wave-train contains significant regions of separated flow which travel downstream and the wave-breaking occurs in a travelling frame whilst the structures seen in Figs. 6 and 7 are practically stationary with respect to the wall. In addition the secondary eruption is seen to occur much sooner in this second context and it is hard to separate it from the generation of pressure max/min which occurs in the short-scaled interaction. These two observations may be connected as the theory summarised in Sect. 4.2 predicts that, initially at least, the pressure disturbance has only a weak interaction with the wall-layer, which remains governed by linear dynamics, as it moves downstream with speed c given by (25). For lower values of c, which might arise for velocity profiles with an inflection point close to the wall, we might expect the interaction to be stronger and perhaps in this case we might expect the wall-eruptions to occur before the incursion of

wall-normal pressure gradients and vortex generation. Thus an analysis of the effects of small values of c in the theoretical approach may well be worthwhile.

6 Conclusion

James Lighthill's original paper is a fascinating read and in this article we have not concentrated on many of the additional results on the details of the flow structure in shock reflection which it contains. Instead, we have emphasized the fundamental physical mechanism, the viscous pressure–displacement interaction, which it was the first to identify, although the original paper does not present it in these terms explicitly. It is clear that this mechanism has found remarkable application in varied areas of fluid mechanics and especially in the challenging and fundamentally important areas of flow transition and separation. It has become a cornerstone in an asymptotic high-Reynolds number theory of steady and unsteady boundary-layer flows which has been developed since the original paper was published and which has extended Prandtl's original theory.

Sections 4.3 and 5.2 on the computation of finite-Reynolds-number flows and their interpretation in terms of the asymptotic theory show the necessity of such an interpretation being performed very carefully. Lighthill emphasised the need to consider problems with parameters within a realistic range and to interpret any asymptotics with care. Indeed, he noted this in a paper (62), published posthumously, and which reviews his original work on upstream influence from a historical viewpoint.

Acknowledgements The author wishes to thanks to Frank Smith and Kevin Cassel for valuable discussions on the content of this paper.

References

1. Prandtl L (1905) Über Flüsskigkeitsbewegung bei sehr kleiner Reibung. In: Vehr. III. Intern Math Kongr Heidelberg, pp 484–491
2. Goldstein S (1930) Concerning some solutions of the boundary-layer equations in hydrodynamics. Proc Camb Phil Soc 26:1–30
3. Goldstein S (1948) On laminar boundary-layer flow near a position of separation. Quart J Mech Appl Math 1:43–69
4. Stewartson K (1969) On the flow near the trailing edge of a flat plate. Mathematika 16:106–121
5. Messiter AF (1970) Boundary-layer flow near the trailing edge of a flat plate. SIAM J Appl Math 18:241–257
6. Neiland VYa (1969) Towards a theory of separation of the laminar boundary layer in a supersonic stream. Izv Akad Nauk SSSR, Mekh Zhidk i Gaza 4:53–57
7. Stewartson K (1970) Is the singularity at separation removable? J Fluid Mech 44:347–364
8. Stewartson K (1981) D'Alembert's paradox. SIAM Rev 23:308–343
9. Lighthill MJ (1953) On boundary layers and upstream influence. II. Supersonic flows without separation. Proc Roy Soc London (A217):478–507
10. Lighthill MJ (1950) Reflection at a laminar boundary layer of a weak steady disturbance to a supersonic stream, neglecting viscosity and heat conduction. Quart J Mech Appl Math 3:303–325
11. Stewartson K (1951) On the interaction between shock waves and boundary layers. Proc Camb Phil Soc 47:545–553
12. Lighthill MJ (1958) Introduction to Fourier analysis and generalised functions. Cambridge University Press
13. Van Dyke M (1964) Perturbation methods in fluid mechanics. Academic Press, New York
14. Kaplun S (1957) Low Reynolds number flow past a circular cylinder. J Math Mech 6:595–603
15. Lagerstrom PA, Cole PA (1955) Examples illustrating expansion proceedures for the Navier-Stokes equations. J Rat Mech Anal 4:817–882
16. Lighthill MJ (1949) A technique for rendering approximate solutions to physical problems uniformly valid. Phil Mag 40:1179–1201
17. Smith FT (1976) Flow through constricted or dilated pipes and channels: Part 1. Quart J Mech Appl Math 29:343–364
18. Smith FT (1976) Flow through constricted or dilated pipes and channels: Part 2. Quart J Mech Appl Math 29:365–376
19. Gajjar J, Smith FT (1983) On hypersonic free interactions, hydraulic jumps and boundary layers with algebraic growth. Mathematika 30:77–93
20. Bowles RI, Smith FT (1992) The standing hydraulic jump: theory, computations and comparisons with experiments. J Fluid Mech 242:145–168

21. Stewartson K, Williams PG (1969) Self-induced separation. Proc Roy Soc London 312:181–206
22. Smith FT (1977) The laminar separation of an incompressible fluid streaming past a smooth surface. Proc Roy Soc London A365:433–463
23. Smith FT (1986) Steady and unsteady boundary-layer separation. Ann Rev Fluid Mech 18:197–220
24. Tollmien W (1929) Über die entstehung der Turbulenz. Nach Ges Wiss Göttingen, pp 79–114
25. Lin CC (1946) On the stability of two-dimensional parallel flows. Quart Appl Math 3:117–142, 213–234, 277–301
26. Smith FT (1979) On the non-parallel flow stability of the Blasius boundary layer. Proc Roy Soc London A366:91–109
27. Smith FT (1979) Nonlinear stability of boundary layers for disturbances of various sizes. Proc Roy Soc London 368: 573–589
28. Rosenhead L (1963) Laminar boundary layers. Dover Publications, New York
29. Hoyle JM, Smith FT (1994) On finite-time break-up in three-dimensional unsteady interacting boundary layers. Proc Roy Soc London A447:467–492
30. Stewart PA, Smith FT (1987) The resonant-triad nonlinear interaction in boundary-layer transition. J Fluid Mech 179: 227–252
31. Smith FT, Walton AG (1989) Nonlinear interaction of near-planar TS waves and longitudinal vortices in boundary-layer transition. Mathematika 36:262–289
32. Stewart PA, Smith FT (1992)Three-dimensional nonlinear blow-up from a nearly planar initial disturbance in boundary-layer transition; theory and experimental comparisons. J Fluid Mech 244:649–676
33. Sandham ND, Kleiser L (1992) The late stages of transition to turbulence in channel flow. J Fluid Mech 245:319–348
34. Kachanov YS (1994) Physical mechanisms of laminar-boundary-layer transition. Ann rev Fluid Mech 26:411–482
35. Bake S, Fernholz HH, Kachanov YS (2000) Resemblance of K- and N- regimes of boundary-layer transition at late stages. Eur J Mech B Fluids 19(1):1–22
36. Han G, Tumin A, Wygnanski I (1999) Laminar-turbulent transition in Poiseuille pipe flow subjected to periodic perturbation emanating from the wall. Part 2. Late stage of transition. J Fluid Mech 419:1–27
37. Smith FT (1988) Finite-time break-up can occur in any unsteady interacting boundary layer. Mathematika 35:256–373
38. Smith FT and Bowles RI (1992) Transition theory and experimental comparisons on (a) amplification into streets and (b) a strongly nonlinear break-up criterion. Proc Roy Soc London A439:163–175
39. Li L, Walker JDA, Bowles RI, Smith FT (1998) Short-scale break-up in unsteady interactive layers: local development of normal pressure gradients and vortex wind-up. J Fluid Mech 374:335–378
40. Bowles RI (2000) Transition to turbulent flow in aerodynamics. Phil Trans Roy Soc London 358:245–260
41. Smith FT, Bowles RI, Walker JDA (2000) Wind-up of a spanwise vortex in deepening transition and stall. Theoret Comput Fluid Dynamics 14:135–165
42. Bowles RI (2000) On vortex interaction in the latter stages of boundary-layer transition. In: Fasel H, Saric WS (eds) Laminar-turbulent transition, IUTAM Symposium, Sedona, Arizona, USA, 1999. Springer-Verlag, Berlin, pp 275–280
43. Whitham GB (1974) Linear and nonlinear waves. Wiley-Interscience, New York
44. Lighthill MJ (2004) Waves in fluids. Cambridge University Press
45. Marshall TJ (2004) A study of three-dimensional effects in end-stage boundary layer transition. PhD thesis, University College London
46. Bowles RI, Davies C, Marshall JT, Smith FT (2005) Stall, transition and turbulence: a tribute to JDAW. *AIAA paper 2005-4934.* Presented at 4th AIAA Theoretical Fluid Mechanics Meeting, Toronto, Canada, 6–9 June 2005
47. Ryzhov OS (2006) Transition length in turbine/compressor blade flows. Proc Roy Soc London A462:2281–2298
48. Bowles RI, Davies C, Smith FT (2003) On the spiking stages in deep transition and unsteady separation. J Eng Math 45:227–245
49. van Dommelen LL, Shen SF (1980) The spontaneous generation of the singularity in a separating laminar boundary layer. J Comput Phys 38:125–140
50. van Dommelen LL (1981) Unsteady boundary-layer separation. PhD thesis, Cornell University, Ithaca, NY
51. Cowley SJ (1983) Computer extension and analaytic continuation of Blasius' expansion for impulsive flow past a cylinder. J Fluid Mech 135:389–405
52. Elliott JW, Cowley SJ, Smith FT (1983) Breakdown of boundary layers: (i) on moving surfaces; (ii) in semi-similar unsteady flow; (iii) in fully unsteady flow. Geophys Astrophys Fluid Dyn 25:77–138
53. Cassel KW, Smith FT, Walker JDA (1996) The onset of instability in unsteady boundary-layer separation. J Fluid Mech 315:223–256
54. Obabko AV, Cassel KW (2000) Large-scale and small-scale interaction in unsteady separation. In: Fluids 2000, Denver Colorado, June 19–22, number AIAA Paper 2000–2469
55. Cassel KW (2000) A comparison of Navier–Stokes solutions with the theoretical description of unsteady separation. Phil Trans Roy Soc London A 358:3207–3227
56. Brinkman KW, Walker JDA (2001) Instability in a viscous flow driven by streamwise vortices. J Fluid Mech 432:127–166
57. Obabko AV, Cassel KW (2002) Navier–Stokes solutions of unsteady separation induced by a vortex. J Fluid Mech 465:99–130
58. Obabko AV, Cassel KW (2005) On the ejection-induced instability in Navier–Stokes solutions of unsteady separation. Phil Trans Roy Soc London A 363:1189–1198

59. Obabko AV, Cassel KW A Rayleigh instability in a vortex induced unsteady boundary layer. J Fluid Mech (To be published)
60. Bodonyi RJ, Smith FT (1985) On the short-scale inviscid instabilities in flow past surface-mounted obstacles and other parallel motions. Aero J (June/July):205–212
61. Cowley SJ (2000) Laminar boundary-layer theory: a 20th century paradox? In: Aref H, Phillips JW (eds) Proc 20th Int Congr of Theoret and Appl Mech, Chicago, IL, pp 389–411
62. Lighthill MJ (2000) Upstream influence in boundary layers 45 years ago. Phil Trans Roy Soc London 358:3047–3061